Applied Physics Reviews ARTICLE scitation.org/journal/are

Mexican-hat potential energy surface in two-dimensional III_2-VI_3 materials and the importance of entropy barrier in ultrafast reversible ferroelectric phase change

Cite as: Appl. Phys. Rev. **8**, 031413 (2021); doi: 10.1063/5.0056695
Submitted: 13 May 2021 · Accepted: 4 August 2021 ·
Published Online: 3 September 2021

Yu-Ting Huang,[1] Nian-Ke Chen,[1] Zhen-Ze Li,[1] Xian-Bin Li,[1,a)] Xue-Peng Wang,[1] Qi-Dai Chen,[1] Hong-Bo Sun,[1,2,a)] and Shengbai Zhang[3,a)]

AFFILIATIONS

[1]State Key Laboratory of Integrated Optoelectronics, College of Electronic Science and Engineering, Jilin University, Changchun 130012, China

[2]State Key Laboratory of Precision Measurement Technology and Instruments, Department of Precision Instrument, Tsinghua University, Beijing 100084, China

[3]Department of Physics, Applied Physics, and Astronomy, Rensselaer Polytechnic Institute, Troy, New York 12180, USA

[a)]**Authors to whom correspondence should be addressed:** lixianbin@jlu.edu.cn; hbsun@tsinghua.edu.cn; and zhangs9@rpi.edu

ABSTRACT

First-principles calculations reveal a Mexican-hat potential energy surface (PES) for two-dimensional (2D) In_2Se_3. This unique PES leads to a pseudo-centrosymmetric paraelectric β phase that resolves the current controversy between theory and experiment. We further show that while the α-to-β (ferroelectric-to-paraelectric) phase transition is fast and coherent, assisted by an in-plane shear phonon mode, a random distribution of the atoms in the trough of the PES acts as an entropy barrier against the reverse β-to-α transition. This will be the origin of the speed limitation of current In_2Se_3 ferroelectric devices. However, if one orders the β phase (due to the formation of in-plane ferroelectric domains), the reverse transition can take place within tens of picoseconds in the presence of a perpendicular electric field. Finally, the Mexican-hat PES is a general feature for the entire family of 2D III_2-VI_3 materials. Our finding offers a critical physical picture in controlling the ultrafast reversible phase transition in 2D In_2Se_3 and other III_2-VI_3 materials, which will benefit their practical industrial development for advanced ferroelectric devices.

I. INTRODUCTION

Because of the spontaneous-aligned electric dipole, which can be switched reversibly by an external electric field, ferroelectric materials have been utilized for applications in capacitors, actuators, sensors, and nonvolatile memories.[1–8] However, in traditional ABO_3 perovskite-type ferroelectric materials, the strength of the spontaneous polarization is hampered by an enhancement of the depolarization field, when its size is scaled down to several nanometers.[9–11] As such, it is challenging for nanoscale integration of ferroelectric devices based on traditional materials, which has limited the development of high-density ferroelectric memory. Very recently, a new kind of two-dimensional (2D) van der Waals layered material, In_2Se_3, has emerged as a potential solution for low-dimensional ferroelectrics due to its intrinsic ferroelectric polarization at the nanoscale, down to the limit of even a monolayer,[12] such as its applications in the scalable synaptic ferroelectric semiconductor junction,[13] the ferroelectric semiconductor field-effect transistor,[7] and the memory-and-neural-computing system.[6]

The α phase of 2D In_2Se_3 holds an out-of-plane ferroelectric polarization at room temperature.[14] When above the Curie temperature (at 700 K), In_2Se_3 will undergo a transition from the (ferroelectric) α phase to the (paraelectric) β phase.[15] The atomic structure and ferroelectricity of the α phase have been firmly identified.[14,16–20] However, those of the β phase have not, e.g., even the understanding of its atomic structure has been controversial. For example, Ding *et al.* suggested that the centrosymmetric β phase is energetically unstable and will therefore exist in the form of a non-centrosymmetric structure with the middle-layer Se atoms moving away from the central positions.[12] As a result, the β phase should have an in-plane ferroelectric

polarization. On the other hand, based on the second-harmonic generation (SHG) spectroscopy, Xiao *et al.* showed that the intensity of the SHG signals of the α phase drops rapidly as the sample temperature rises to 700 K. The α-to-β phase transition therefore should result in a paraelectric phase in the centrosymmetric structure.[19] In our view, the disagreement stems from a lack of atomic-scale dynamic study of the finite-temperature phase transition. This may also hinder a precise control of material properties for device applications, such as the current slow writing speed of In_2Se_3 ferroelectric memory.[4]

In this research, based on first-principles calculations and *ab initio* molecular dynamics (MD), we identify a unique Mexican-hat potential energy surface (PES) for the middle layer Se atoms in 2D In_2Se_3 for the first time. This results in a pseudo-centrosymmetric paraelectric phase where the centrosymmetry of the middle Se layer is broken at any moment, but the centrosymmetry is preserved on average at the macroscopic level. Our finding resolves the current controversy between theory and experiment. Importantly, we show that the α-to-β phase transition is assisted by a shear phonon mode, while the reverse β-to-α transition is blocked by a random distribution of the Se atoms. This will be the origin of the speed limitation of current In_2Se_3 ferroelectric devices. One need to control the motion of the Se atoms to overcome the entropy barrier, which leads to an accelerated β-to-α transition in a matter of only tens of picoseconds, in the presence of a vertical electric field. Last, we show that the Mexican-hat PES is a general feature for the entire family of 2D III_2-VI_3 ferroelectric materials. The results offer a critical dynamics picture of III_2-VI_3 materials for their advanced ferroelectric applications.

II. RESULTS AND DISCUSSION

A monolayer In_2Se_3 consists of five atomic layers that alternate in a sequence of Se-In-Se-In-Se, and atoms in each atomic layer form a triangular lattice.[21] Figure 1(a) shows the atomic structure of the (ferroelectric) α phase.[12] In particular, there are two kinds of In atoms, one in the top (*t*) layer and the other in the bottom (*b*) layer—each In(*t*) atom forms a tetrahedral configuration with four nearest neighbor (NN) Se atoms, while each In(*b*) atom forms an octahedral configuration with six NN Se atoms. The ferroelectricity is a result of the spontaneous polarization due to the unequal environments between In(*t*) and In(*b*). In comparison, Fig. 1(b) shows the atomic structure of the (paraelectric) β phase, where both In(*t*) and In(*b*) forms octahedra with their NN Se atoms. This symmetric arrangement forces the middle layer Se [Se(*m*)] atoms to be at the centrosymmetric positions. Here, we denote the (centrosymmetric) β phase as β_c. Unlike the usual displacement-type ferroelectric mechanism,[22] when ferroelectric transition takes place here, the Se(*m*) atoms of α phase will be displaced considerably, which result in the breaking of old bonds and the making of new bonds of different kinds to form β phase. This re-bonding mechanism explains why α In_2Se_3 can withstand the depolarization field, even when the thickness is only one monolayer.[12] Figures 1(c) and 1(d) show the calculated phonon spectra, which supports the notion that the α phase is dynamically stable. In contrast, the β_c phase is unstable, showing a significant number of imaginary frequencies.

To understand the instability of β phase, one ought to consider the PES of the ions as PES determines atomic vibrations and subsequently the phonon spectrum. Figures 2(a) and 2(b) compare the in-plane PES for Se atoms [following the convention for In atoms, these Se atoms are demoted as Se(*t*), Se(*b*), and Se(*m*), respectively]. Due to

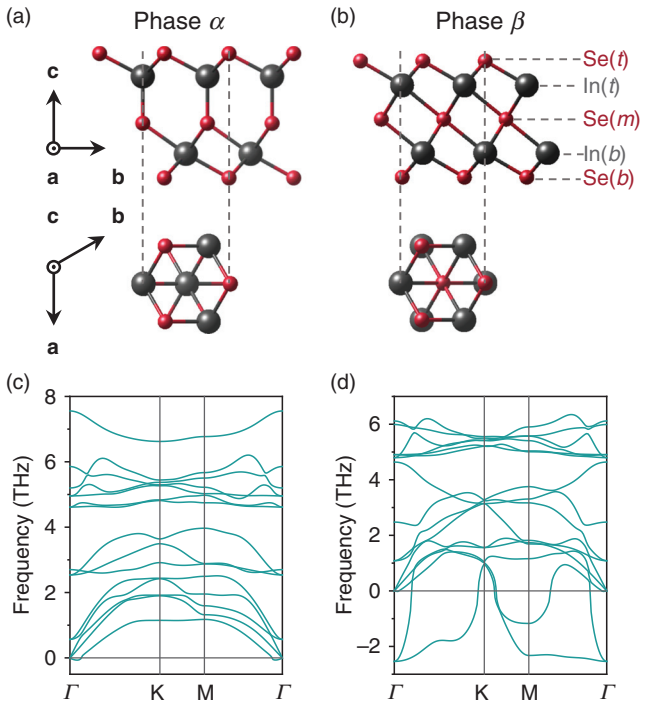

FIG. 1. Side and top views of (a) ferroelectric state (α phase) and (b) paraelectric state (centrosymmetric β phase, i.e., β_c) of 2D In_2Se_3. Both phases contain five atomic sublayers. The Se atom in the middle layer is referred to as Se(*m*). The Se and In atoms on the top and bottom layers are called Se(*t*), In(*t*), Se(*b*), and In(*b*), respectively. (c–d) Phonon spectra of α In_2Se_3 and β In_2Se_3 at 0 K shows that the β_c phase is actually unstable with the appearance of significant imaginary frequencies.

the inversion symmetry of the β_c phase, the PES for Se(*t*) is identical to that for Se(*b*). The PES of Se(*t* or *b*) exhibits a single minimum at the standard lattice position. However, the PES of Se(*m*) is markedly different, as it exhibits a Mexican-hat profile, as can be seen clearly in Fig. 2(b). To be precise, there are in fact 12 local energy minima in the basin of the Mexican-hat PES, which can be classed into three types with distinct bonding topologies: 3 for B site, 6 for C site, and 3 for D site, as shown in Figs. 2(b) and 2(c). We name the β phases with particular (in-plane) off-center atomic displacement of the Se(*m*) atoms the $\beta_{ip}(k)$ phases, where k = B, C, and D. Phonon calculations in Note 1 of the supplementary material confirm that, at these 12 energy minima, the imaginary frequencies in Fig. 1(d) for the β_c phase are eliminated.

As it appears, a realization of the β_{ip} phases is difficult, because there are 12 off-center positions with similar energies, and the energy barriers between them are also small. When taking into account entropy contribution to the free energy at high temperature, it is less likely that such long-range ordered β_{ip} phase can exist. As such, the β phase at elevated temperature is expected to be a β with a random distribution of the Se(*m*) atoms inside the valley of the Mexican-hat PES.

Such a β phase can be obtained from the α phase by raising the temperature, for example, when $T > 700$ K.[19,23] To investigate such a finite temperature effect, we resort to *ab initio* MD. Figure 3 shows an example of the β phase over a 20-ps MD run at 750 K. Its free energy and mean square displacement as functions of time are shown in

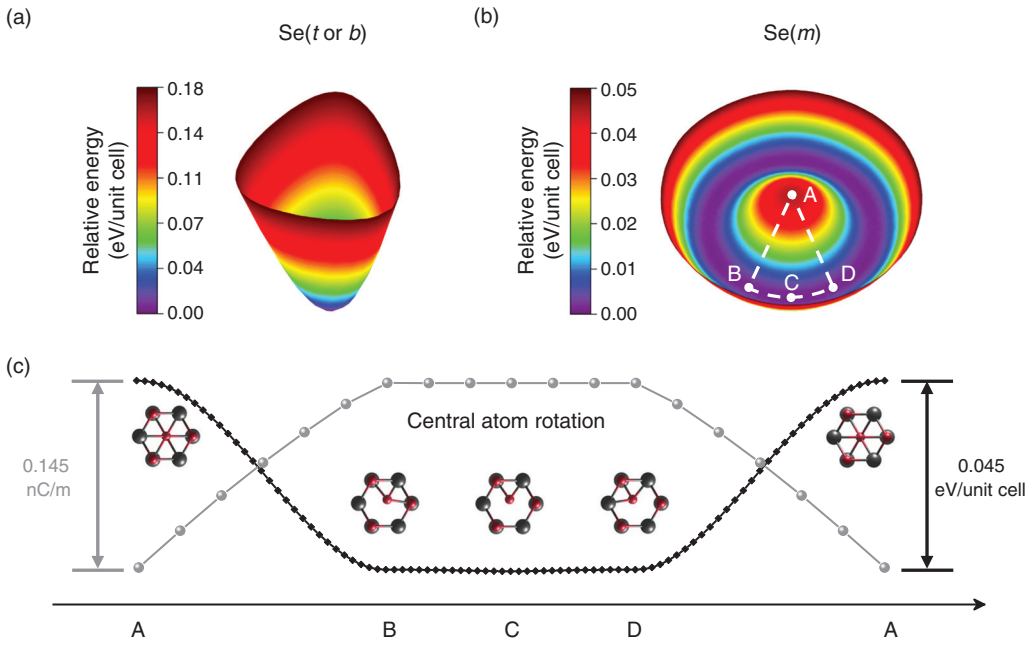

FIG. 2. Potential energy surfaces (PESs) of (a) Se(t or b) and (b) Se(m) in the in-plane direction of β phase of 2D In_2Se_3. For a unit cell, the PES of a single Se atom is calculated by sampling its coordinates in the x-y plane with other four atoms fixed. (c) The in-plane polarization intensity (gray curve) and energy (black curve) along four specific sites (A-B-C-D-A) from the Mexican-hat PES, where A represents the center of honeycomb and B, C, D are the quasi-stationary points with energy minimum as shown in (b).

Fig. 3(a). For such a dynamic system, a typical structure (e.g., at $t = 7$ ps) and the corresponding locally relaxed structure are shown in Fig. 3(b), left and right, respectively. Clearly, the Se(m) atoms prefer the off-center sites, instead of the centrosymmetric A site, in line with the PES analyses above. As we have speculated, these off-center sites are randomly distributed along the basin of the Mexican-hat PES. Two additional transient structures, and the corresponding relaxed structures, at $t = 0$ and 5 ps are given in Note 2 of the supplementary material, which also support the conclusion above. Figure 3(c) (left) shows the time averaged structure, in which the trajectories of the Se(m) atoms are shown. These trajectories suggest that the Se(m) atoms follow a random walk within a region centered at the centrosymmetric A site. As such, the time-averaged structure is representative of the pseudo-centrosymmetric β phase or called β_{pc}. This agrees with the SHG experiment.[19]

Figures 3(d)–3(f) plot the probability of in-plane distributions of Se atoms, namely, Se(t), Se(m), and Se(b), during the 20-ps MD simulation. The origin represents the standard lattice site and a in the coordinate axis is the side length of the in-plane hexagonal lattice. It shows that the distributions of the Se(t) and Se(b) atoms form relatively sharp domes, centered at the corresponding Se atomic sites, while that of the Se(m) atoms are more diffusive and hence a relatively flat dome. These differences are a consequence of the difference of the PESs for Se(t or b) and Se(m) in Figs. 2(a) and 2(b). Note 3 of the supplementary material provides further discussions to elucidate the causal relation between the Mexican-hat PES and distribution probability. All these indicate Se(m) atoms will induce large entropy in the β_{pc} phase. Note that such a β_{pc} phase could also be retained at room temperature (see the analysis in Note 4 of the supplementary material).

Currently, it is not possible to apply 2D In_2Se_3 for high-speed data memory unless fast switching between opposite polarizations can be realized. The β_{pc} phase with a unique Mexican-hat PES, as an intermediate state between the ferroelectric (↑)→ paraelectric → ferroelectric (↓) transition and vice versa, plays a decisive role in ultrafast ferroelectric switching. Generally speaking, the switching includes two parts: α-to-β and β-to-α transitions. The first part can be realized simply by increasing temperature. For example, Figs. 4(a) and 4(b) show that an initial α phase can be converted to a β phase in 4 ps at 750 K. Analysis of atomic displacement in the x and y directions in Figs. 4(d) and 4(e) reveals a highly concerted displacement between the In(t) and Se(t) atoms and between the In(b) and Se(b) atoms, while the displacement of the Se(m) atoms correlate with those in the bottom layers but to a smaller degree. As a matter of fact, these results reflect a highly coherent motion of the atoms in which when the two top layers move in the positive x- (or y-) direction, the two bottom layers and the middle layer move in the negative x- (or y-) direction.

Figure 4(f) plots the projected displacements for all 12 optical phonon modes of 2D α phase, as a function of time. The projected displacement here is defined as time integration of the projected velocity for various phonon modes from 0 to t. Details on the calculation can be found in Note 5 of the supplementary material. We see from Fig. 4(f) that, while the displacements of most of the phonon modes oscillate around zero, one of the in-plane shear phonon mode, however, evolves during the transition almost monotonically from zero to having a positive displacement. Accordingly, Fig. 4(c) shows the direction of the atomic displacements for this shear phonon mode. From the side view in Fig. 4(c), it is clear that the displacements consist of in-phase and out-of-phase motions of atomic layers leading to the phase

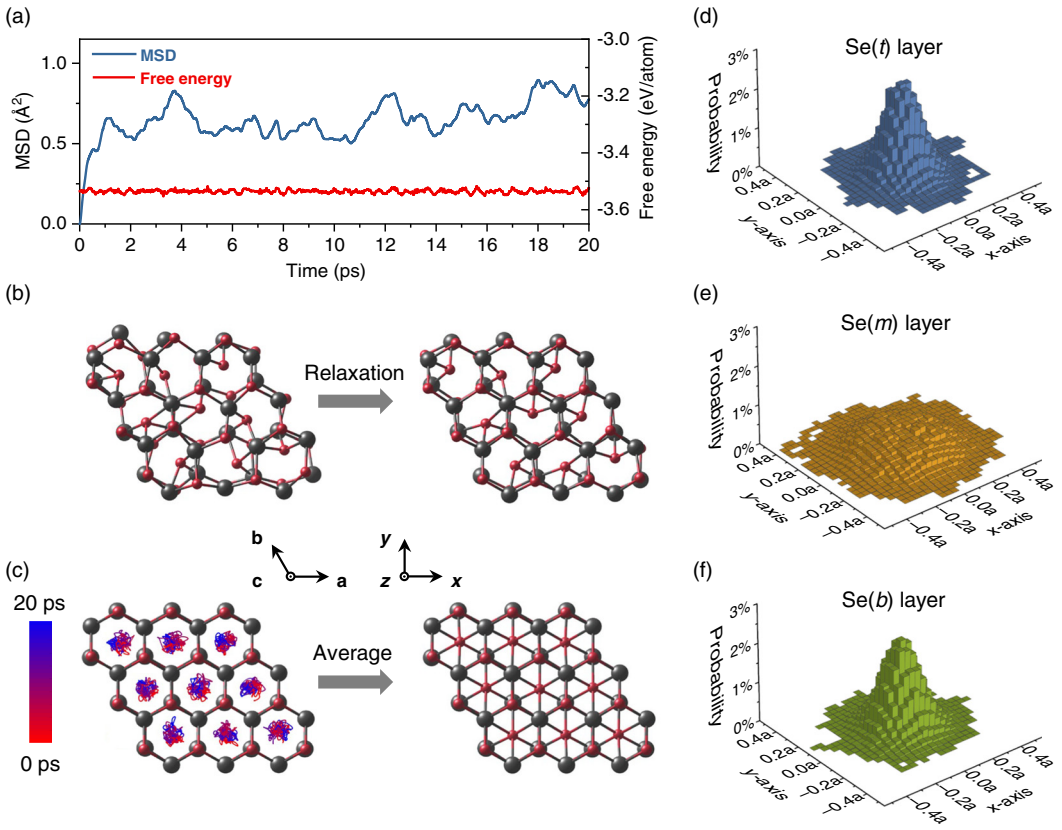

FIG. 3. Characterization of β phase of 2D In_2Se_3 by a 20-ps molecular dynamics (MD) at an elevated temperature of 750 K. (a) Time evolution of mean square displacement (MSD) and free energy. (b) Top view of a snapshot at 7 ps (left), and the corresponding relaxed structure (right). (c) (left) Trajectories of the Se(m) atoms and (right) their average positions. (d–f) Distribution probabilities of Se(t), Se(m), and Se(b) atoms during the MD. Horizontal axes are in unit of the side length of the in-plane hexagonal lattice, a.

transition. Hence, the ultrafast α-to-β transition is a result of coherent motion of atoms induced by the in-plane shear phonon mode, which only requires that the temperature is sufficiently high.

While the α-to-β transition is fast and direct, the reverse β-to-α transition in a short time can be more difficult, even when an out-of-plane electric field (in the polarization direction of the α phase) is applied. That is because the random walk of Se(m) atoms in the β_{pc} phase sets a large entropy barrier for the reverse transition due to the Mexican-hat PES. Here, the entropy barrier can be estimated by the distribution probability of Se atoms during MD simulations. For example, compared to the case of 2D Sb_2Te_3, which does not possess the Mexican-hat PES, the contribution of the Mexican-hat PES to the free energy of 2D β_{pc} In_2Se_3 at 750 K is –80 meV per unit cell or equivalently an entropy barrier of 1.07×10^{-4} eV/K per unit cell (see Note 6 of the supplementary material for calculation details). This will be the origin of the speed limitation of current In_2Se_3 ferroelectric devices.

In order to characterize the α and β phases during the transition, we define a parameter θ that is the angle between an In(t)-Se(m) bond and the basal plane formed by the three In(b) atoms underneath the Se(m) atom [as shown in the inset of Fig. 5(a)]: In the β_c phase, $\theta = 39°$ but in the α phase, $\theta = 90°$. Figure 5(a) shows the probability distribution of θ as a function of time at 300 K and under an out-of-plane electric field of 5 V/nm starting with the β_{pc} phase. For the pseudo-centrosymmetric β_{pc} phase, the distribution exhibits a steady Gaussian shape centered at about 48°. Figure 5(b) shows the result of another MD run under the condition except starting with an ordered distribution of the Se(m) atoms, e.g., in one β_{ip}(B) phase. In contrast to Fig. 5(a), the peak position shifts significantly from about 52° to 76° within 15 ps, and it is accompanied by a narrowing of the θ distribution, demonstrating the successful β_{ip}-to-α transition. If one reverses the direction of the electric field, a β_{ip}-to-α transition with opposite polarization will quickly result as well. As a comparison, current ferroelectric transition of In_2Se_3 by an electric field is still at the timescale from tens of nanosecond to millisecond.[4,6] Phase transition at our simulation timescale is not perfect with residue defects, see Note 7 of the supplementary material. In our structural analysis, these defects have been excluded.

As ordering the Se(m) atoms into one of the off-center B, C, and D phases is the key for fast reverse β-to-α transition, it is important to understand under what condition(s), such an ordering can be physically realized. In this regard, it is important to note that some of the ordered phases have been observed at room temperature by experiment.[24,25] One possibility is a long-range order due to in-plane ferroelectricity, as the experiment has indeed observed ordered domains. Note that for periodic supercells, such a long-range order is absent. To study them, we resort to the Berry phase approach and find that the off-

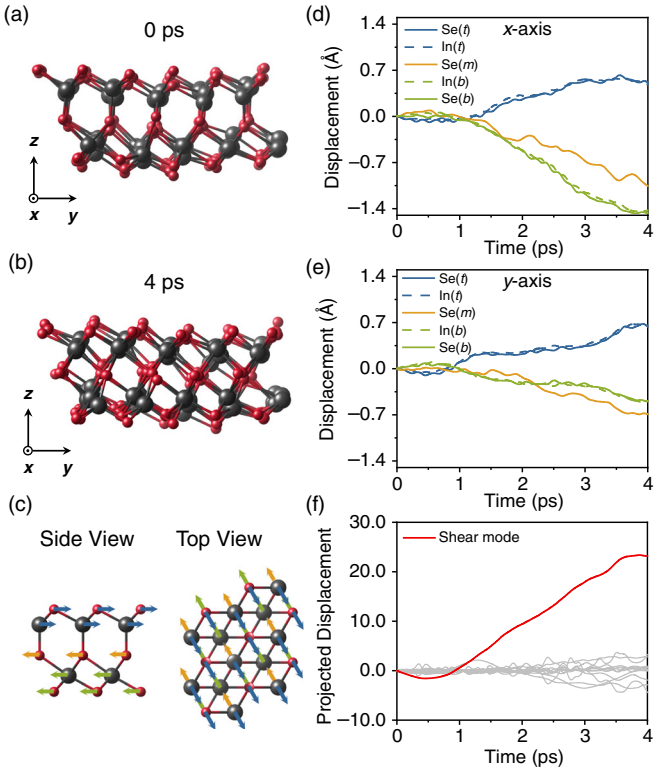

FIG. 4. A fast α-to-β phase transition in 2D In_2Se_3 induced by a shear phonon mode at 750 K. (a) Initial and (b) final structures from the transition within 4 ps. (c) Schematic of the shear phonon mode in α phase to trigger the transition. The arrows indicate the motion directions of atoms in different layers during the transition. (d) and (e) are atomic displacements along *x* and *y* directions during the transition, respectively. (f) Time evolution of atomic displacement projected onto the 12 optical phonon modes of 2D α phase during the transition, where the case related to the shear mode is highlighted by red color.

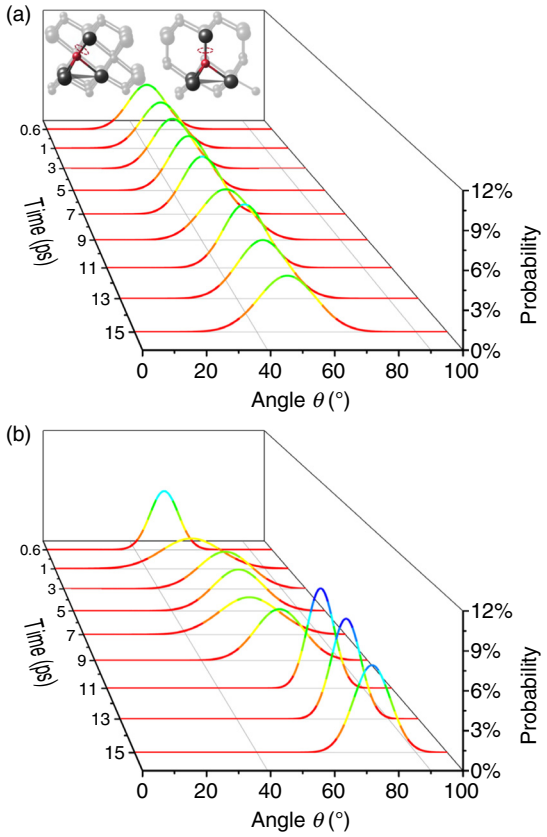

FIG. 5. β-to-α transition in 2D In_2Se_3 in the presence of an out-of-plane electric field of 5 V/nm along the c axis, as revealed by a 15-ps MD at 300 K. The transition is characterized by the bond angle (θ) between the encircled In(*t*)-Se(*m*) bond and the basal plane of the three In(*b*) atoms underneath the Se(*m*) [see the inset of panel (a) with highlighting the bond and the basal plane]. (a) Starting with the β_{pc} phase with a random Se(*m*) distribution and (b) starting from β_{ip}(B) phase but with a coherent in-plane Se(*m*) distribution. In the actual calculation, we obtain the initial β_{ip}(B) phase at 0 K, then we raise the temperature to 300 K in 1 ps, followed by 14-ps MD at fixed temperature.

center β_{ip} phases have the same polarization intensity of 0.145 nC/m. This can lead to macroscopic electric field and ordered domains of finite size, as the strength of the field in 2D will diminish when the separation between the charges (located on opposing edges) is too large.

It is also worth noting that the Mexican-hat PES of the β phase is a general phenomenon of the 2D III_2-VI_3 family (III = Al, Ga, In; and VI = S, Se, Te), as shown in Fig. 6. The top views of the corresponding atomic structures are shown in the insets, while the side views and lattice constant *l* are summarized, respectively, in Note 8 of the supplementary material. Similar to In_2Se_3, all III_2-VI_3 hold the double-well energy profile for the VI(*m*) atoms. Note 9 of the supplementary material lists the calculated energy barriers at the central positions. The calculated phonon spectra in Note 10 of the supplementary material further reinforce the notion that the centrosymmetric β_c phase is unstable. All these support other 2D III_2-VI_3 materials have the similar atomic picture as In_2Se_3 has.

III. CONCLUSIONS

In summary, by first-principles calculations and MD simulations, we reveal a Mexican-hat PES for 2D In_2Se_3 and, as a matter of fact, for the entire family of 2D III_2-VI_3 ferroelectric compounds. Due to the unique PES, a new form of the β phase is identified as the pseudo-centrosymmetric β_{pc} phase, where the Se(*m*) atoms take random off-center positions but time-averaged to be centrosymmetric. This random motion effectively creates an entropy barrier that hinders a fast β-to-α transition, which will be the origin of the speed limitation of current In_2Se_3 ferroelectric devices. This is contrasted to the α-to-β transition, which is ultrafast at elevated temperature due to coherent atomic motions under a shear phonon mode. By overcoming the entropy barrier via ordering the atoms in the β phase, the β-to-α transition can happen just within tens of picoseconds with the help of an out-of-plane electric field. Furthermore, due to the absence of a high-temperature melting process as in phase-change Ge-Sb-Te alloy,[26–28] the energy consumption of In_2Se_3 to encode data could be potentially lower. Our study thus offers a new angle on the physics of ferroelectric transitions, namely, the need to overcome the entropy barrier, which should benefit the development of future ferroelectric data storage at ultrafast speed and ultrathin scale.

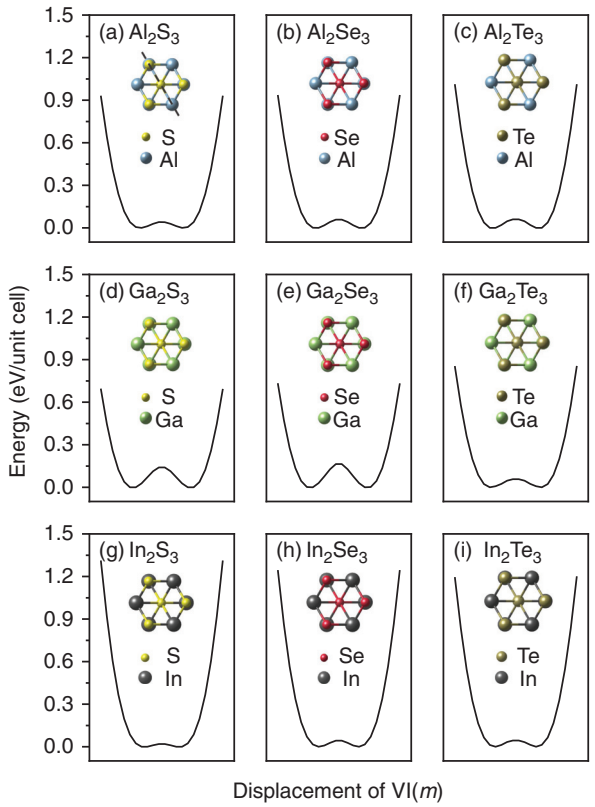

FIG. 6. Universal Mexican-hat PES for the family of 2D III_2-VI_3 compounds. The line plot of the PES has been carried out along the diagonal line shown in the inset of (a). (a) Al_2S_3, (b) Al_2Se_3, (c) Al_2Te_3, (d) Ga_2S_3, (e) Ga_2Se_3, (f) Ga_2Te_3, (g) In_2S_3, (h) In_2Se_3, and (i) In_2Te_3.

IV. COMPUTATIONAL METHODS

Calculations were performed based on density functional theory (DFT) using the Vienna *ab initio* simulation package.[29,30] The projector augmented wave pseudopotential[31] and Perdew-Burke-Ernzerhof exchange correlation functional[32] were used. The energy cutoff for the plane wave expansion was set to 275 eV. A $16 \times 16 \times 1$ Monkhorst-Pack[33] k-point grid was used for structural relaxation. A 20 Å vacuum region in the vertical direction was incorporated to minimize the effect of periodic boundary. The *z*-dimension of the supercell was fixed when performing the structural relaxation. Phonon band structures were calculated using the PHONOPY code.[34] To obtain the PES of a Se atom in 2D β In_2Se_3, we uniformly sample the in-plane positions of a Se atom, while keeping other atoms fixed in a unit cell. The total energies of these configurations are then calculated by self-consistent DFT calculations. For each PES calculation, 1180 Se positions were used. Berry phase method[35] was used to estimate the in-plane polarization. The external electric field was realized by introducing a dipole field perpendicular to the monolayer In_2Se_3 with a strength of 5 V/nm. MD simulations were preformed using the *NVT* ensemble[36] and a $7 \times 7 \times 1$ supercell containing 245 atoms. A Γ-point sampling of the Brillouin zone was used with the MD time step of 1 fs.

SUPPLEMENTARY MATERIAL

See the supplementary material for more details, Notes 1–10.

AUTHORS' CONTRIBUTIONS

Y.T.H., N.K.C., and Z.Z.L. performed the calculations and contributed equally to this article. X.B.L., Y.T.H., Z.Z.L., N.K.C., and S.Z. did the theoretical analysis. The paper is written by Y.T.H., X.B.L., and S.Z. with the help of other authors. X.B.L. and H.B.S. proposed and initiated the project. Y.T.H., N.K.C., and Z.Z.L. contributed equally to this work.

ACKNOWLEDGMENTS

Work in China was supported by the National Natural Science Foundation of China (Grants Nos. 61922035, 11904118, 11874171, and 61775077), the Fundamental Research Funds for the Central Universities, and China Postdoctoral Science Foundation (2019M661200). S.Z. was supported by the U.S. Department of Energy under Award No. DE-SC0002623. The High-Performance Computing Center (HPCC) at Jilin University for computational resources is also acknowledged.

DATA AVAILABILITY

The data that supports the findings of this study are available within the article and its supplementary material.

REFERENCES

[1]C. A. P. De Araujo, J. D. Cuchiaro, L. D. McMillan, M. C. Scott, and J. F. Scott, Nature **374**, 627 (1995).
[2]S. L. Miller, R. D. Nasby, J. R. Schwank, M. S. Rodgers, and P. V. Dressendorfer, J. Appl. Phys. **68**, 6463 (1990).
[3]J. F. Scott and C. A. Paz de Araujo, Science **246**, 1400 (1989).
[4]S. Y. Wan, Y. Li, W. Li, X. Y. Mao, C. Wang, C. Chen, J. Y. Dong, A. M. Nie, J. Y. Xiang, Z. Y. Liu, W. G. Zhu, and H. L. Zeng, Adv. Funct. Mater. **29**, 1808606 (2019).
[5]X. Tao and Y. Gu, Nano Lett. **13**, 3501 (2013).
[6]S. Wang, L. Liu, L. Gan, H. Chen, X. Hou, Y. Ding, S. Ma, D. W. Zhang, and P. Zhou, Nat. Commun. **12**, 53 (2021).
[7]M. W. Si, A. K. Saha, S. J. Gao, G. Qiu, J. K. Qin, Y. Q. Duan, J. Jian, C. Niu, H. Y. Wang, W. Z. Wu, S. K. Gupta, and P. D. Ye, Nat. Electron. **2**, 580 (2019).
[8]N. Setter, D. Damjanovic, L. Eng, G. Fox, S. Gevorgian, S. Hong, A. Kingon, H. Kohlstedt, N. Y. Park, G. B. Stephenson, I. Stolitchnov, A. K. Taganstev, D. V. Taylor, T. Yamada, and S. Streiffer, J. Appl. Phys. **100**, 051606 (2006).
[9]J. Junquera and P. Ghosez, Nature **422**, 506 (2003).
[10]T. Birol, Nature **560**, 174 (2018).
[11]C. H. Ahn, K. M. Rabe, and J. M. Triscone, Science **303**, 488 (2004).
[12]W. Ding, J. Zhu, Z. Wang, Y. Gao, D. Xiao, Y. Gu, Z. Zhang, and W. Zhu, Nat. Commun. **8**, 14956 (2017).
[13]M. Si, Y. Luo, W. Chung, H. Bae, D. Zheng, J. Li, J. Qin, G. Qiu, S. Yu, and P. Ye, IEEE International Electron Devices Meeting (IEDM) (IEEE, 2019) pp. 130–133.
[14]Y. Zhou, D. Wu, Y. Zhu, Y. Cho, Q. He, X. Yang, K. Herrera, Z. Chu, Y. Han, M. C. Downer, H. Peng, and K. Lai, Nano Lett. **17**, 5508 (2017).
[15]J. van Landuyt, G. van Tendeloo, and S. Amelinckx, Phys. Status Solidi A **30**, 299 (1975).
[16]L. Debbichi, O. Eriksson, and S. Lebègue, J. Phys. Chem. Lett. **6**, 3098 (2015).
[17]C. Cui, F. Xue, W.-J. Hu, and L.-J. Li, NPJ 2D Mater. Appl. **2**, 18 (2018).
[18]C. J. Cui, W. J. Hu, X. G. Yan, C. Addiego, W. P. Gao, Y. Wang, Z. Wang, L. Z. Li, Y. C. Cheng, P. Li, X. X. Zhang, H. N. Alshareef, T. Wu, W. G. Zhu, X. Q. Pan, and L. J. Li, Nano Lett. **18**, 1253 (2018).

[19]J. Xiao, H. Zhu, Y. Wang, W. Feng, Y. Hu, A. Dasgupta, Y. Han, Y. Wang, D. A. Muller, L. W. Martin, P. Hu, and X. Zhang, Phys. Rev. Lett. **120**, 227601 (2018).
[20]F. Xue, J. Zhang, W. Hu, W.-T. Hsu, A. Han, S.-F. Leung, J.-K. Huang, Y. Wan, S. Liu, J. Zhang, J.-H. He, W.-H. Chang, Z. L. Wang, X. Zhang, and L.-J. Li, ACS Nano **12**, 4976 (2018).
[21]K. Osamura, Y. Murakami, and Y. Tomiie, J. Phys. Soc. Jpn. **21**, 1848 (1966).
[22]G. A. Samara, T. Sakudo, and K. Yoshimitsu, Phys. Rev. Lett. **35**, 1767 (1975).
[23]J. Liu and S. T. Pantelides, 2D Mater. **6**, 025001 (2019).
[24]C. X. Zheng, L. Yu, L. Zhu, J. L. Collins, D. Kim, Y. D. Lou, C. Xu, M. Li, Z. Wei, Y. P. Zhang, M. T. Edmonds, S. Q. Li, J. Seidel, Y. Zhu, J. Z. Liu, W. X. Tang, and M. S. Fuhrer, Sci. Adv. **4**, eaar7720 (2018).
[25]C. Xu, Y. Chen, X. Cai, A. Meingast, X. Guo, F. Wang, Z. Lin, T. W. Lo, C. Maunders, S. Lazar, N. Wang, D. Lei, Y. Chai, T. Zhai, X. Luo, and Y. Zhu, Phys. Rev. Lett. **125**, 047601 (2020).
[26]M. Zhu, K. Ren, L. Liu, S. Lv, X. Miao, M. Xu, and Z. Song, Phys. Rev. Mater. **3**, 033603 (2019).
[27]X.-B. Li, X. Q. Liu, X. Liu, D. Han, Z. Zhang, X. D. Han, H.-B. Sun, and S. B. Zhang, Phys. Rev. Lett. **107**, 015501 (2011).
[28]Z. R. Wang, H. Q. Wu, G. W. Burr, C. S. Hwang, K. L. Wang, Q. F. Xia, and J. J. Yang, Nat. Rev. Mater. **5**, 173 (2020).
[29]G. Kresse and J. Furthmüller, Phys. Rev. B **54**, 11169 (1996).
[30]G. Kresse and J. Furthmüller, Comput. Mater. Sci. **6**, 15 (1996).
[31]G. Kresse and D. Joubert, Phys. Rev. B **59**, 1758 (1999).
[32]J. P. Perdew, K. Burke, and M. Ernzerhof, Phys. Rev. Lett. **78**, 1396 (1997).
[33]M. Methfessel and A. T. Paxton, Phys. Rev. B **40**, 3616 (1989).
[34]A. Togo and I. Tanaka, Scr. Mater. **108**, 1 (2015).
[35]R. D. King-Smith and D. Vanderbilt, Phys. Rev. B **47**, 1651 (1993).
[36]S. Nosé, J. Chem. Phys. **81**, 511 (1984).